

DOI:10.5281/zenodo.2557280

CZU 620.3:621.315.55



## ENHANCEMENT IN UV SENSING PROPERTIES OF ZnO:Ag NANOSTRUCTURED FILMS BY SURFACE FUNCTIONALIZATION WITH NOBLE METALIC AND BIMETALLIC NANOPARTICLES

Vasile Postica,<sup>1</sup> Alexander Vahl,<sup>2</sup> Nicolae Magariu,<sup>1</sup> Maik-Ivo Terasa,<sup>3</sup> Mathias Hoppe,<sup>3</sup> Bruno Viana,<sup>4</sup> Patrick Aschehoug,<sup>4</sup> Thierry Pauporté,<sup>4</sup> Ion Tiginyanu,<sup>5</sup> Oleksandr Polonskyi,<sup>2</sup> Victor Sontea,<sup>1</sup> Lee Chow,<sup>6</sup> Lorenz Kienle,<sup>7</sup> Rainer Adelung,<sup>3</sup> Franz Faupel,<sup>2</sup> Oleg Lupan,<sup>1,3,4,\*</sup>

<sup>1</sup> Department of Microelectronics and Biomedical Engineering, Center Nanotechnology and Nanosensors, Technical University of Moldova, 168 Stefan cel Mare Av., MD-2004 Chisinau, Republic of Moldova

<sup>2</sup> Chair for Multicomponent Materials, Institute for Materials Science, Kiel University, Kaiserstr. 2, D-24143, Kiel, Germany

<sup>3</sup> Functional Nanomaterials, Institute for Materials Science, Kiel University, Kaiserstr. 2, D-24143, Kiel, Germany

<sup>4</sup> PSL University, Chimie ParisTech-CNRS, Institut de Recherche de Chimie Paris, UMR8247, 11 rue P. et M. Curie, 75005 Paris, France

<sup>5</sup> Institute of Electronic Engineering and Nanotechnology, MD-2028 Chisinau, Republic of Moldova

<sup>6</sup> Department of Physics, University of Central Florida, Orlando, FL 32816 USA

<sup>7</sup> Institute for Materials Science – Synthesis and Real Structure, Faculty of Engineering, Christian-Albrechts-University of Kiel, Kaiserstraße 2, D-24143 Kiel, Germany

\*Corresponding author: Lupan Oleg, E-mail: [ollu@tf.uni-kiel.de](mailto:ollu@tf.uni-kiel.de) [oleg.lupan@mib.utm.md](mailto:oleg.lupan@mib.utm.md)

Received: June, 18, 2018

Accepted: October, 14, 2018

**Abstract.** In this study, Ag-doped ZnO (ZnO:Ag) nanostructured films were functionalized with silver nanoparticles (Ag NPs), silver-platinum bimetallic nanoparticles (AgPt NPs) and silver-gold bimetallic NPs (AgAu NPs) using a gas phase PVD process based on a Haberland type gas aggregation cluster source and unipolar DC planar magnetron sputtering. Ultraviolet (UV) sensing investigations showed a respectable time constants reduction for rising and decaying photocurrents, as well as an increase for the UV response. Compared to a pristine nanostructured film the surface functionalization with Ag, AgPt and AgAu increased the UV response by factors of 2.7, 3.5 and 4, respectively. The increased performances of the here presented ZnO:Ag nanostructured films functionalized with monometallic and bimetallic NPs based photodetectors are explained by the increased lifetime of photogenerated electron – hole pairs, as well as the formation of nanoscale Schottky barriers at the interface of Au/ZnO:Ag and Pt/ZnO:Ag.

**Keywords:** *UV photodetector, zinc oxide, silver nanoparticles, nanostructured films.*

### Introduction

During the past few decades, being among the most important optoelectronic devices, photodetectors based on micro- and nanostructures of metal oxides have received special attention due to their unique electronic and chemical properties, as well as their high surface-to-volume ratio [1-3]. In this context, UV photodetectors play an important

role in flame sensing, advanced communications, ozone sensing, etc. [3, 4]. The high-performance photodetectors generally need to satisfy several requirements: (i) high sensitivity; (ii) high signal-to-noise ratio, (iii) high spectral selectivity; (iv) high speed; (v) high stability [3, 4], etc. Having a wide bandgap of 3.37 eV at room temperature, ZnO micro- and nanostructures are ideal candidates for visible-blind UV photodetectors [5, 6]. Among one-dimensional, two-dimensional and three-dimensional ZnO structures, the ZnO nanostructured films with high surface-to-volume ratio are alternative platforms for constructing photodetectors [3, 4]. A wide range of physical and chemical methods were used for the deposition of nanostructured films, including chemical deposition, metal-organic chemical vapor deposition (MOCVD), pulsed laser deposition (PLD), atomic layer deposition (ALD), magnetron sputtering, etc. [7-10]. However, many of these techniques are sophisticated and need expensive systems. In this context, the deposition of ZnO nanostructured films from chemical solutions at relatively low temperatures combines the advantage of simplicity and low cost. Previously, the Sn-doped and Fe-doped ZnO nanostructured films were deposited on glass substrates via a simple synthesis from chemical solutions (SCS) approach from aqueous baths, and demonstrated high sensitivity but slow response and recovery values under illumination with UV [11, 12]. The latter two present the major obstacles for the usage in high-speed UV photodetectors.

In this work, the Ag-doped ZnO nanostructured films, synthesized via a synthesis from chemical solutions (SCS) approach, were functionalized with monometallic and bimetallic Ag-based NPs, namely Ag, AgPt and AgAu NPs in order to improve the response time of rising and decaying photocurrents. While surface functionalization with AgNPs of ZnO micro- and nanostructures was widely used for the improvement of UV photodetectors performances [13-15], surface functionalization with bimetallic nanoparticles was less reported and needs a comprehensive study, which is the main objective of this investigation.

### Experimental part

The Ag-doped ZnO nanostructured films were deposited on the pre-cleaned glass substrates (commercial microscope glass slides, 76 mm × 25 mm × 1 mm) via a synthesis from chemical solutions (SCS) approach using aqueous baths, as reported previously [9-12]. By adding the 5.3 mM of silver nitrate ( $\text{AgNO}_3$ ) in a complex solution a 0.95 wt% Ag content in ZnO:Ag nanostructured films was achieved. The film thickness of all samples used in this study is  $1.5 \pm 0.2 \mu\text{m}$ . The given thickness was obtained by performing fixed number of SCS cycles. The post-deposition rapid thermal annealing (RTA) at 575 °C for 60 s was applied to all samples. A previous study demonstrated that the RTA treatment at 575 °C for 60 s can greatly enhance the sensing properties of Fe-doped ZnO nanostructured films [12].

The Ag, AgAu, and AgPt NPs depositions on the surface of ZnO nanostructured films was performed via a gas phase PVD process based on a Haberland type gas aggregation cluster source and unipolar DC planar magnetron sputtering [16-19].

The morphological properties of the ZnO:Ag nanostructured films were measured by a Zeiss Ultraplus SEM at 7 kV. The micro-Raman spectroscopy was performed using a WITec alpha 300 RA system [12]. The optical measurements (transmittance, reflectance and diffuse reflectance spectra measurements) were performed with a Cary 5000 UV-Vis-NIR spectrophotometer equipped with an integrating sphere as was reported previously [11, 20]. The photoluminescence (PL) measurements were performed using a YAG:Nd-OPO laser

(EKSPLA) and a HR250 monochromator (Jobin-Yvon), coupled with an UV-enhanced intensified charge-coupled device (ICCD; Roper) [11, 20]. The structure of the elaborated photodetectors was described in detail in our previous work [11]. The electrical and UV sensing properties were measured using a Keithley 2400 SourceMeter, which allows for current measurements with a resolution of 10 pA [11]. The UV light intensity ( $P_{opt}$ ) was set to 1 mW/cm<sup>2</sup> (using a SSEYL Sentry ST-513 UVAB meter). The UV sensing measurements were performed in ambient air with 30% relative humidity (RH) [21].

### Results and discussions

Figure 1a,b shows the SEM images of Ag-doped ZnO nanostructured films with 0.95 wt% Ag and RTA-treated at 575 °C. The film is composed of randomly distributed columnar-like grains with diameters in the range of 100 – 300 nm. Figure 1b discloses that the ZnO grains are partially interconnected. The deposited films are relatively uniform without any formation of agglomerations (see Figure 1a). The SEM images of the Ag NPs-functionalized ZnO:Ag nanostructured films are presented in Figure 1c and 1d. On the surface of the ZnO:Ag grains, randomly distributed NPs with diameter in range of 6 – 12 nm can be seen. Probably due to the homogenous distribution of NPs no percolation paths formation was observed. Figures 1e and 1f show the SEM images of AgPt and AgAu NPs-functionalized on ZnO:Ag nanostructured films, respectively. The AgPt/ZnO:Ag deposition, leads to a formation of NPs clusters, while for the deposition of AgAu/ZnO:Ag bimetals results in a separation of relatively smaller and bigger NPs.

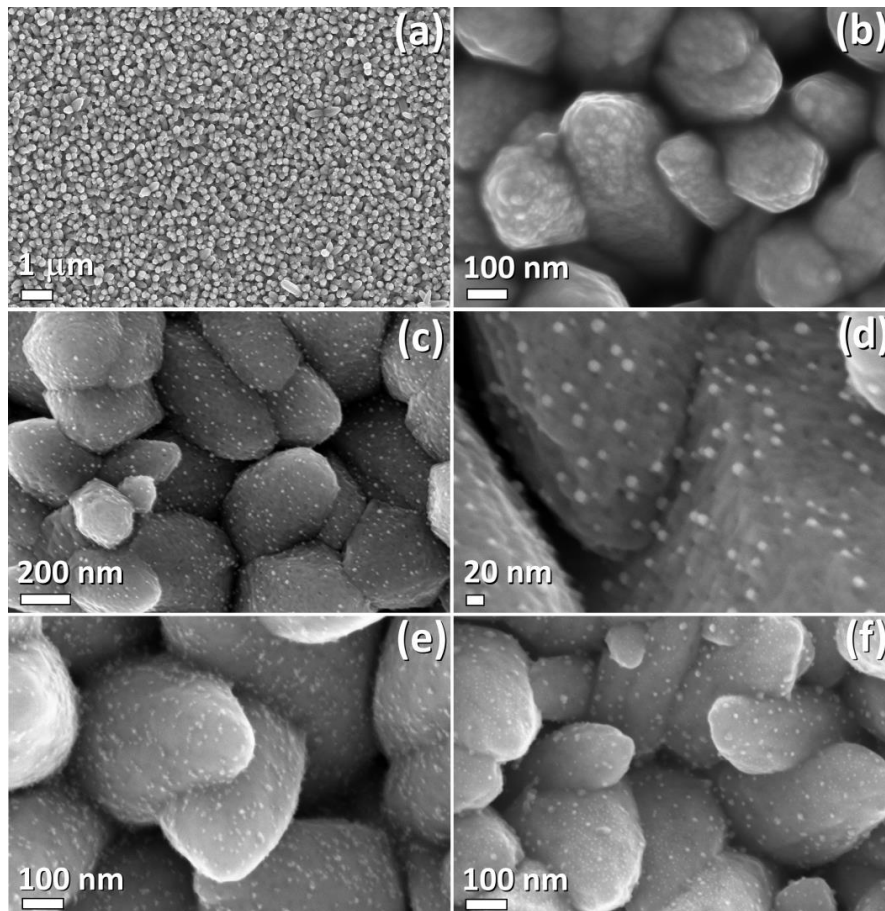


**Figure 1.** SEM images of ZnO:Ag nanostructured films: (a,b) pristine; (c,d) Ag NPs-functionalized; (e) AgPt NPs- functionalized; (f) AgAu NPs- functionalized.

Figure 2a and 2b shows the transmission and absorbance spectra of AgPt/ZnO:Ag nanostructured films. As was reported previously for undoped and Sn-doped ZnO nanostructured films, the transmittance in the visible light region is over 60% [11]. This means the incorporation of AgPt/ZnO:Ag only reduces the transmission of about 15% in region of 400 – 500 nm. The sharp absorption edge from Figure 2b is attributed to the electronic transition of ZnO [22]. The optical band gap energy ( $E_g$ ) was calculated using the Tauc equation [11, 20]:

$$(\alpha h\nu)^2 = B(h\nu - E_g) \quad (1)$$

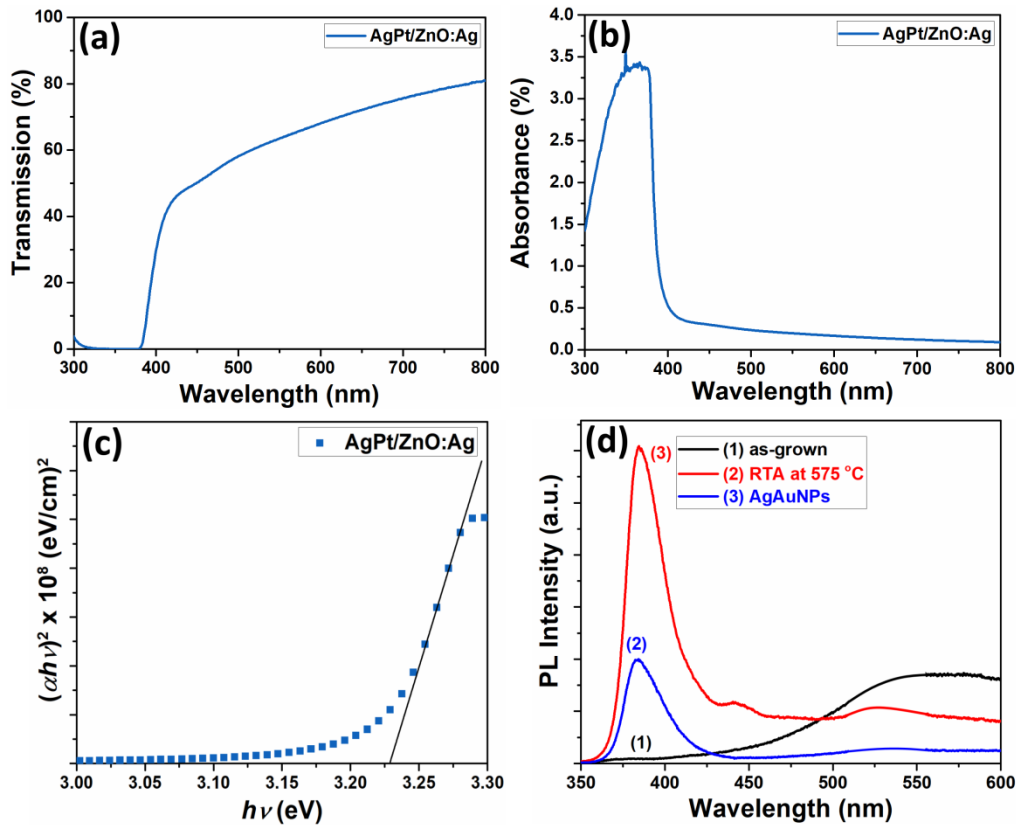
where  $\alpha$  is the absorption coefficient,  $h\nu$  is the incident photon energy, and  $B$  is a material-dependent constant. Figure 2c shows the dependence of  $(\alpha h\nu)^2$  vs.  $h\nu$ . From the intercept of the linear region,  $E_g = 3.22$  eV was obtained.

Figure 2d shows the room temperature PL spectra of as-grown and RTA treated ZnO:Ag nanostructured films, as well as AgAu NPs-functionalized ZnO:Ag samples. The as-grown sample showed mainly one emission, i.e. a broad peak in the region of 460 – 660 nm. Emissions from this region are usually related to the defects such as oxygen vacancies ( $V_o$ ), interstitial oxygen ( $O_i$ ) and interstitial zinc ( $Zn_i$ ), i.e. it demonstrates poor crystallinity and stoichiometry of as-grown films [11, 20, 23]. After the RTA treatment at 575 °C for 60 s, an emission peak at ~ 385 nm appears, which is related to the UV near-band-edge (NBE) emission also the PL-intensity from visible region is reduced [11, 20, 23]. This confirms, as was also demonstrated in previous work for Sn-doped ZnO nanostructures films [11], that the RTA treatment can greatly improve the crystal quality of ZnO nanostructured films, which is very important for UV sensing applications [7, 11, 12, 20, 24]. After surface functionalization with AgAu NPs, the intensity of NBE emission for treated samples is slightly reduced, which states that the electrons and holes are more separated and that the radiative recombination is quenched, i.e. leads to a longer lifetime of photogenerated carriers (which is very important for UV sensing applications), proving the successful surface functionalization with AgAu NPs [25, 26].

Figure 3 shows the room temperature dynamic UV response of ZnO:Ag, Ag/ZnO:Ag, AgPt/ZnO:Ag and AgAu/ZnO:Ag nanostructured films, where the UV response is 17, 46, 60 and 68, respectively (see Figure 4a and Table 1). The UV response was defined as the ratio of photocurrent ( $I_{UV}$ ) vs. dark current ( $I_{dark}$ ). All samples were exposed to UV light for a duration of 120 s. Therefore, it can be concluded that surface functionalization with monometallic and bimetallic noble metal nanoparticles can efficiently improve the UV response of ZnO:Ag nanostructured films, which is more related to the presence of Ag and will be discussed later with UV sensing mechanism. The UV sensing properties of undoped ZnO samples were already reported [11, 12]. Compared to a pristine nanostructured film the surface functionalization with Ag, AgPt and AgAu NPs increased the UV response by a factor of 2.7, 3.5 and 4, respectively.

In the case of pristine samples, an incomplete recovery of decaying photocurrent can be observed, which is widely attributed to the persistent photoconductivity (PPC) due to the presence of surface trapping states/defects in the case of metal oxide nano- and microstructures with a high surface-to-volume ratio. In the case of ZnO these surface trapping states/defects are related usually to ionization of deep and neutral  $V_o$  states to

shallow donor states  $V_O^{\bullet\bullet}$ , which slowly release the captured carriers leading to increased photocarrier lifetime ( $\tau$ ), i.e. slow recovery time [11, 27, 28].



**Figure 2.** (a) Transmission spectra, (b) absorbance spectra and (c) plot of  $(\alpha h\nu)^2$  vs. photon energy ( $h\nu$ ) of AgPt/ZnO:Ag films, (d) room temperature PL spectra.

Figure 2d as well as a previous study demonstrates that thermal treatment in air, especially rapid thermal treatment can reduce the  $V_O$  states and improve the stoichiometry [11, 21]:



where  $O_O$  is the oxygen located at their regular position in the zinc oxide lattice. However, the RTA at 575 °C for 60 s is not enough to considerably reduce the PPC effect.

In order to evaluate more precisely the information about the time constants of rising and decaying photocurrents the bi-exponential fitting was applied [4]:

$$I(t) = I_{dark} + A_1 \left( 1 - e^{-\frac{t}{\tau_{r1}}} \right) + A_2 \left( 1 - e^{-\frac{t}{\tau_{r2}}} \right) \quad (3)$$

$$I(t) = I_{dark} + A_3 e^{-\frac{t}{\tau_{d1}}} + A_4 e^{-\frac{t}{\tau_{d2}}} \quad (4)$$

where  $A_1$ ,  $A_2$ ,  $A_3$  and  $A_4$  are positive constants, while  $\tau_{r1}$ ,  $\tau_{r2}$  and  $\tau_{d1}$ ,  $\tau_{d2}$  are time constants for rising and decaying photocurrent, respectively. The constants  $\tau_{r1}$  and  $\tau_{d1}$  are correlated to the rapid change in photocurrent when UV source is switched on/off, which is related to fast change in the concentration of charge carriers [8, 11, 12, 29].

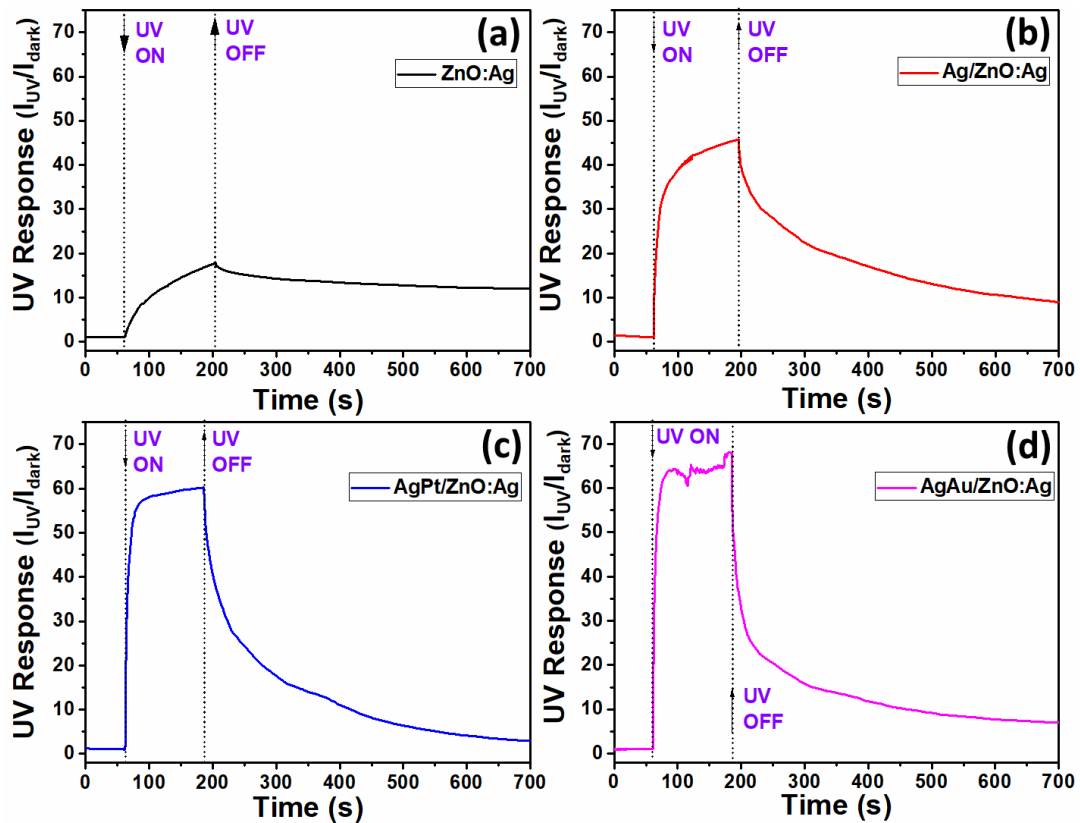


**Figure 3.** The dynamic UV response for: (a) ZnO:Ag; (b) Ag/ZnO:Ag; (c) AgPt/ZnO:Ag and (d) AgAu/ZnO:Ag nanostructured films.

As it was discussed for PPC, the constant  $\tau_{r2}$  and  $\tau_{d2}$  are related to trapping carriers and their release due to the vacancies of oxygen defects, as well as photodesorption/adsorption processes of oxygen molecules (as will be discussed in the section with UV sensing mechanism) [8, 11, 12, 29]. The calculated time constants are presented in Table 1 and Figure 4b. The considerable decrease in time constants by surface functionalization with NPs can be observed, especially for rising photocurrent. For example,  $\tau_{r1}$  is decreasing from 14.46 for ZnO:Ag to 4.48, 3.74 and 0.96 s for Ag/ZnO:Ag, AgPt/ZnO:Ag and AgAu/ZnO:Ag, respectively.

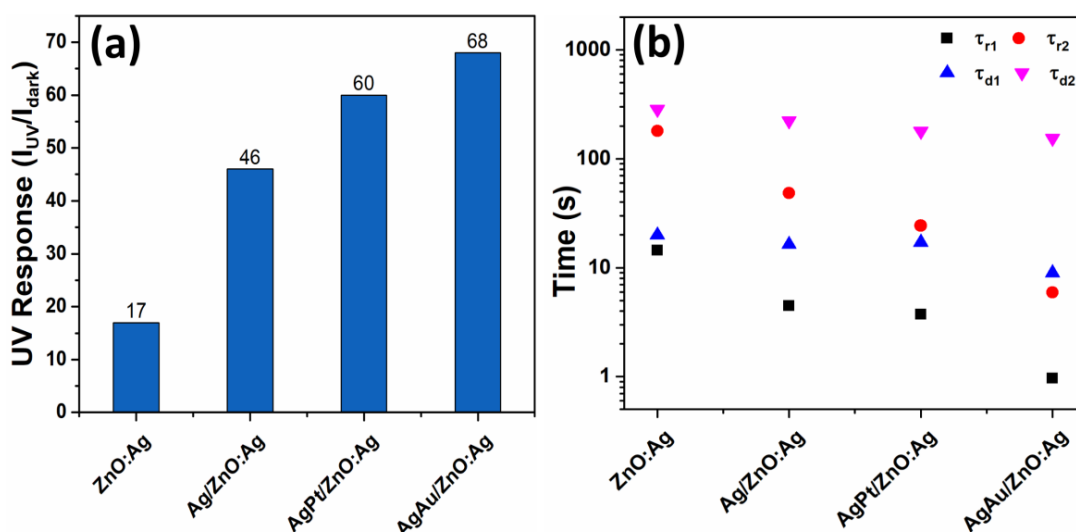


**Figure 4.** (a) UV response for ZnO:Ag; Ag/ZnO:Ag; AgPt/ZnO:Ag and AgAu/ZnO:Ag nanostructured films. (b) The time constants for rising and decaying photocurrents.

Table 1

Time constants for rising and decaying photocurrent					
Sample	UV response ( $I_{UV}/I_{dark}$ )	$\tau_{r1}$ (s)	$\tau_{r2}$ (s)	$\tau_{d1}$ (s)	$\tau_{d2}$ (s)
ZnO:Ag	17	14.46	179.79	19.83	284.0
Ag NPs/ZnO:Ag	46	4.48	48.58	16.28	222.74
AgPt NPs/ZnO:Ag	60	3.74	24.33	17.07	178.54
AgAu NPs/ZnO:Ag	68	0.96	5.94	8.95	154.05

Additional important parameters which determine the performance of photodetectors are the responsivity ( $R$ ) and the internal photoconductive gain ( $G$ ), which were calculated as follows [8, 9, 30-32]:

$$R = \frac{I_{ph}}{P_{opt} \cdot S} = \eta \left( \frac{q\lambda}{hc} \right) G \quad (5)$$

$$G \cong \frac{1}{L^2} \tau \mu_e V \quad (6)$$

where  $q$  is the electron charge,  $I_{ph}$  is photocurrent ( $I_{UV} - I_{dark}$ ),  $P_{opt}$  is the incident optical power (1 mW/cm<sup>2</sup>),  $S$  is the effective area of the photodetector,  $\eta$  is the quantum efficiency (is assumed to be 1, for simplicity),  $h$  is Planck's constant,  $c$  is the speed of light,  $\lambda$  is the wavelength of UV light (365 nm),  $L$  is the distance between the pads (1 mm),  $\mu_e$  is the electron mobility and  $V$  is the applied bias voltage (0.1 V). The calculated parameters are presented in Figure 5. The specific detectivity ( $D^*$ ) is a further figure of merit for photodetectors and can be calculated assuming the dark current to be the major source of shot noise using the expressions [33, 34]:

$$D^* = \frac{R\sqrt{S}}{\sqrt{2qI_{dark}}} \quad (7)$$

The calculated results are presented in Figure 5c. For all enumerated parameters, it can be observed that surface functionalization with monometallic and bimetallic NPs leads to enhancement in performance of ZnO:Ag based photodetectors in the following order: Ag NPs < AgPt NPs < AgAu NPs. However, the  $G < 1$  indicates the absence of photoconductive gain in nanostructured films, which can be attributed to a wide  $L$  (see Eq. (6)) [8, 11, 32]. A detectivity in the range of  $8.6 \times 10^{11}$  -  $9.34 \times 10^{11}$  Jones provides quantitative evidence that functionalized nanostructured films are extremely sensitive to small optical input signals [7].

### UV sensing mechanism of functionalized ZnO:Ag nanostructured films

The UV sensing mechanism based on doped ZnO nanostructured films was proposed in previous works [11, 12]. In this work, we will focus mainly on the effect of surface functionalization of ZnO:Ag with NPs. The general sensing mechanism is based on adsorption of oxygen molecules on the surface of ZnO:Ag grains [8, 15]:



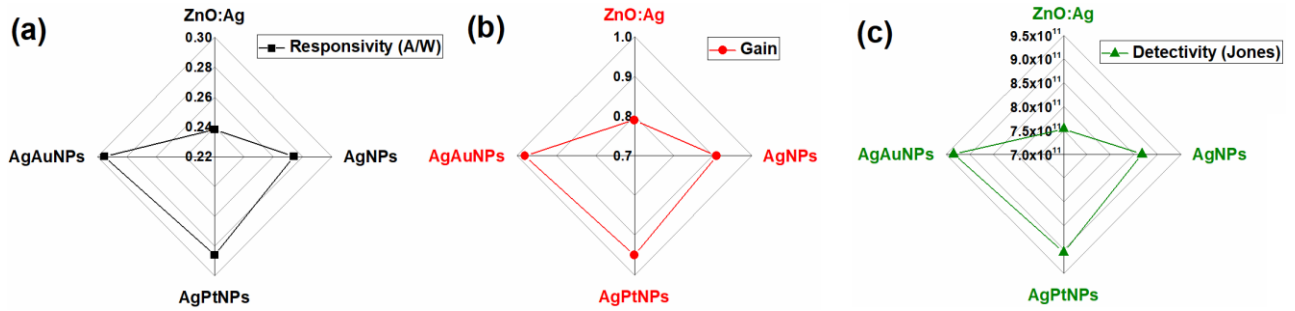


**Figure 5.** The calculated parameters of photodetectors based on ZnO:Ag nanostructured films: (a) Responsivity (A/W); (b) Photoconductive gain; and (c) Detectivity (Jones).

These reactions lead to capture of free electrons from ZnO:Ag grains and the creation of an electron depletion region at the surface with higher resistivity [15]. This will lead to a formation of potential barriers between grains [12]. In this case, the conductance of a grain network is [35]:

$$G \propto \frac{q\mu_e N_d (D-W)^2}{L} \exp\left(-\frac{qV_s}{kT}\right) \quad (10)$$

where  $D$  is the grains diameter,  $W$  is the width of electron depletion region,  $T$  is the absolute temperature,  $V_s$  is the surface potential and  $N_d$  is the donor concentration within the grain. Therefore, the current which flows between the grains is dependent mainly on the width and the height of the contact potential barriers [11, 12, 35]. Under exposure to UV light, electron-hole ( $e^- + h^+$ ) pairs are generated in the ZnO:Ag grains ( $E = h\nu \rightarrow e^- + h^+$ ) [15]. The photo-generated pairs are separated by the built-in electric field ( $V_s$ ) in the electron depleted layer ( $W$ ) [8, 15]. The photo-generated holes migrate to the surface of the grains to recombine with electrons from adsorbed oxygen molecules (which lead to desorption of oxygen molecules) and narrowing of electron depletion region:



The unpaired electrons are left in the conduction region of the grains and significantly contribute to the increase in the photocurrent of the photodetector structure [8, 15].

The considerable performances enhancement of the ZnO:Ag films by surface functionalization with Ag NPs can be explained as follows. The work function of Ag (4.26 eV) is smaller than that of ZnO (5.2 eV) [36]. Therefore, electrons will migrate from Ag to the conduction band ( $E_c$ ) of ZnO to achieve the Fermi level equilibrium when they get in contact with each other Ag/ZnO:Ag ( $Ag \rightarrow Ag^+ + e^-$ ) [36, 37]. Under UV illumination, the rapid transfer of photogenerated electrons to Ag NPs will considerably increase the lifetime ( $\tau$ ) of the photogenerated pairs [36, 38], and therefore will increase the photodetector performance (see Eq. (5-8)). This also explains the considerably decreased time constants for Ag NPs-functionalized samples. The presence of Ag NPs improves the surface reactions involving adsorption, dissociation, and the ionization of oxygen in the presence of Ag NPs [36, 37]. Negatively charged surface oxygen at the surface of Ag NPs can facilitate the transfer of electrons or of the negatively charged adsorbed oxygen,  $O_2^-$ , to the surface of ZnO:Ag during the recovery reaction [36, 37].



The surface functionalization with bimetallic NPs, i.e. AgAu NPs and AgPt NPs, leads to noticeable performance improvements of the photodetectors while compared to samples functionalized with monometallic Ag NPs are only minor enhancements can be confirmed (see Figure 5). This can indicate that the main improvements are achieved using Ag NPs, while Au and Pt NPs provide only slightly further improvements. The work function of Pt (5.9 eV) is larger than that of ZnO, which leads to the formation of nanoscale Schottky barriers at the interface of Pt/ZnO [24, 38-39]. This will lead to the widening of the electron depletion region under Pt NPs, and further to a higher modulation of potential barrier height under UV illumination, i.e. higher UV response [24]. The highest performances of AuAg NPs-functionalized ZnO:Ag nanostructured films can be explained based on increased light absorption efficiency induced by light scattering of Au NPs [24].

## Conclusions

We have demonstrated that surface functionalization of Ag-doped ZnO nanostructured films with monometallic and bimetallic Ag-based nanoparticles can essentially improve the performance of ZnO photodetectors. The UV response of ZnO:Ag nanostructured films increased by factor of 2.7, 3.5 and 4 for functionalization with Ag NPs, AgAu NPs and AgPt NPs, respectively. The essential reduction in time constants of rising and decaying photocurrent was also observed. While pristine ZnO:Ag nanostructured films demonstrated the presence of PPC due to ionization of neutral  $V_o$  states to shallow donor states  $V_o^{\bullet}$ . This slowly releases the captured carriers from these deep levels. Functionalized samples showed a recovery of more than 90% of total photocurrent on reasonable timescales. This is very important for practical applications, especially in the case of fast detection of UV irradiation. The improved performance of functionalized samples was explained based on the increased lifetime of photogenerated electron – hole pairs, as well as the formation of Schottky barriers which leads to a higher modulation of potential barriers under UV illumination.

**Acknowledgments.** Dr. Lupan acknowledges the Alexander von Humboldt Foundation for the research fellowship and for advanced researches 3-3MOL/1148833 STP at the Institute for Materials Science, Kiel University, Germany. This research was sponsored partially by the German Research Foundation (DFG) under the schemes PAK 902 (KI 1263/14-1 & AD 183/16-1) and by Project SFB859. The authors gratefully acknowledge financial support by the DFG through the research units FOR2093, FOR1616, SCHU 926/25-1 and AD 183/17-1. This research was partly supported by the STCU and ASM within the Grant 6229.

## References

1. Lupan, O.; Koussi-Daoud, S.; Viana, B.; Pauporté, T. Oxide planar p-n Heterojunction Prepared by Low Temperature Solution Growth for UV-Photodetector Application. In: *RSC Advances*, 2016 (6), pp. 68254-60.
2. Gedamu, D.; Paulowicz, I.; Kaps, S.; Lupan, O.; Wille, S.; Haidarschin, G.; Mishra Y., K.; Adelung, R. Rapid Fabrication Technique for Interpenetrated ZnO Nanotetrapod Networks for Fast UV Sensors. In: *Advanced Materials*, 2013, 26 (10), pp. 1541-50.
3. Chen, H.; Liu, H.; Zhang, Z.; Hu, K.; Fang, X. Nanostructured Photodetectors: From Ultraviolet to Terahertz. In: *Advanced Materials*, 2015, 28 (3), pp. 403-33.
4. Chen, H.; Liu, K.; Hu, L.; Al-Ghamdi, AA.; Fang, X. New concept ultraviolet photodetectors. In: *Materials Today*, 2015, 18 (9), pp. 493-502.
5. Liu, X.; GU, L.; Zhang, Q.; Wu, J.; Long, Y.; Fan, Z. All-printable band-edge modulated ZnO nanowire photodetectors with ultra-high detectivity. In: *Nature Communications*, 2014, 5 pp. 4007.

6. Soci, C.; Zhang, A.; Xiang, B.; Dayeh, S.A.; Aplin, Dpr.; Park, J.; Bao, Xy.; Lo, Y.H.; Wang, D. ZnO Nanowire UV Photodetectors with High Internal Gain. In: *Nano Letters*, 2007, 7 (4), pp. 1003-9.
7. Djuricic, A.B.; Chen, X.; Leung, Y.H.; Man Ching N.G, A. ZnO nanostructures: growth, properties and applications. In: *Journal of Materials Chemistry*, 2012, 22 (14), pp. 6526-35.
8. Zhong LIN, W. Zinc oxide nanostructures: growth, properties and applications. In: *Journal of Physics: Condensed Matter*, 2004, 16 (25), pp. R829.
9. Lupan, O.; Shyshyanu, S.; Shyshyanu, T. Nanostructured zinc oxide gas sensors by successive ionic layer adsorption and reaction method and rapid photothermal processing. In: *Thin Solid Films*, 2008, 516 pp. 3338-3345.
10. Lupan, O.; Chow, L.; Shyshyanu, S.; Monaico, E.; Shyshyanu, T.; Sontea, V.; Roldan Cuenya, B.; Naitabi, A.; Park, S.; Schulte, A. Nanostructured zinc oxide films synthesized by successive chemical solution deposition for gas sensor applications. In: *Materials Research Bulletin*, 2009, 44 pp. 63-69.
11. Postica, V.; Hoppe, M.; Gröttrup, J.; Hayes, P.; Röbisch, V.; Smazna, D.; Adelung, R.; Viana, B.; Aschehoug, P.; Pauporté, T.; Lupan, O. Morphology dependent UV photoresponse of Sn-doped ZnO microstructures. In: *Solid State Sciences*, 2017, 71 pp. 75-86.
12. Postica, V.; Hölken, I.; Schneider, V.; Kaidas, V.; Polonskyi, O.; Cretu, V.; Tighinyanu, I.; Faupel, F.; Adelung, R.; Lupan, O. Multifunctional device based on ZnO:Fe nanostructured films with enhanced UV and ultra-fast ethanol vapour sensing. In: *Materials Science in Semiconductor Processing*, 2016, 49 pp. 20-33.
13. Wang, X.; Liu, K.; Chen, X.; Li, B.; Jiang, M.; Zhang, Z.; Zhao, H.; Shen, D. Highly Wavelength-Selective Enhancement of Responsivity in Ag Nanoparticle-Modified ZnO UV Photodetector. In: *ACS Applied Materials & Interfaces*, 2017, 9 (6), pp. 5574-9.
14. Zeng, Y.; Pan, X.; Dai, W.; Chen, Y.; YE, Z. The enhancement of a self-powered UV photodetector based on vertically aligned Ag-modified ZnO nanowires. In: *RSC Advances*, 2015, 5 (82), pp. 66738-41.
15. Lupan, O.; Cretu, V.; Postica, V.; Ahmadi, M.; Cuenya, B.R.; Chow, L.; Tighinyanu, I.; Viana, B.; Pauporté, T.; Adelung, R. Silver-doped zinc oxide single nanowire multifunctional nanosensor with a significant enhancement in response. In: *Sensors and Actuators B: Chemical*, 2016, 223 pp. 893-903.
16. Haberland, H.; KARRAIS, M.; MALL, M.; THURNER, Y. Thin films from energetic cluster impact: A feasibility study. In: *Journal of Vacuum Science & Technology A*, 1992, 10 (5), pp. 3266-71.
17. Solář, P.; Polonskyi, O.; Olbricht, A.; Hinz, A.; Shelemin, A.; Kylián, O.; Choukourov, A.; Faupel, F.; Biederman, H. Single-step generation of metal-plasma polymer multicore@shell nanoparticles from the gas phase. In: *Scientific Reports*, 2017, 7, pp. 8514.
18. Polonskyi, O.; Peter, T.; Ahadi, A.M.; Hinz, A.; Strunskus, T.; Zaporojtchenko, V.; Biederman, H.; Faupel F. Huge increase in gas phase nanoparticle generation by pulsed direct current sputtering in a reactive gas admixture. In: *Applied Physics Letters*, 2013, 103, pp. 033118.
19. Vahl, A.; Strobel, J.; Reichstein, W.; Polonskyi, O.; Strunskus, T.; Kienle, L.; Faupel, F. Single target sputter deposition of alloy nanoparticles with adjustable composition via a gas aggregation cluster source. In: *Nanotechnology*, 2017, 28 (17), pp. 175703.
20. Lupan, O.; Pauporté, T.; Chow, L.; Viana, B.; Pellé, F.; Ono, L.K.; Roldan Cuenya, B.; Heinrich, H. Effects of annealing on properties of ZnO thin films prepared by electrochemical deposition in chloride medium. In: *Applied Surface Science*, 2010, 256 (6), pp. 1895-907.
21. Gröttrup, J.; Postica, V.; Smazna, D.; Hoppe, M.; Kaidas, V.; Mishra, Y.K.; Lupan, O.; Adelung, R. UV detection properties of hybrid ZnO tetrapod 3-D networks. In: *Vacuum*, 2017, 146 pp. 492-500.
22. Wei, Y.; Kong, J.; Yang, L.; Ke, L.; Tan, Hr.; Liu, H.; Huang, Y.; Sun, Xw.; Lu, X.; Du, H. Polydopamine-assisted decoration of ZnO nanorods with Ag nanoparticles: an improved photoelectrochemical anode. In: *Journal of Materials Chemistry A*, 2013, 1 (16), pp. 5045-52.
23. Vanheusden, K.; Seager, C.; Warren, W.T.; Tallant, D.; Voigt, J. Correlation between photoluminescence and oxygen vacancies in ZnO phosphors. In: *Applied physics letters*, 1996, 68 (3), pp. 403-5.
24. Liu, K.; Sakurai, M.; Liao, M.; Aono, M. Giant Improvement of the Performance of ZnO Nanowire Photodetectors by Au Nanoparticles. In: *The Journal of Physical Chemistry C*, 2010, 114 (46), pp. 19835-9.
25. Georgekutty, R.; Seery, M.K.; Pillai, S.C. A Highly Efficient Ag-ZnO Photocatalyst: Synthesis, Properties, and Mechanism. In: *The Journal of Physical Chemistry C*, 2008, 112 (35), pp. 13563-70.
26. Ansari, S.A.; Khan, M.M.; Ansari, M.O.; Lee, J.; Cho, M.H. Biogenic Synthesis, Photocatalytic, and Photoelectrochemical Performance of Ag-ZnO Nanocomposite. In: *The Journal of Physical Chemistry C*, 2013, 117 (51), pp. 27023-30.

27. Jeon, S.; Ahn, S-E.; Song, I.; Kim, C.J.; Chung, U.; Lee, E.; Yoo, I.; Nathan, A.; Lee, S.; Ghaffarzadeh, K.; Robertson, J.; Kim, K. Gated three-terminal device architecture to eliminate persistent photoconductivity in oxide semiconductor photosensor arrays. In: *Nature Materials*, 2012, 11 pp. 301.
28. Gu, X.; Zhang, M.; Meng, F.; Zhang, X.; Chen, Y.; Ruan, S. Influences of different interdigital spacing on the performance of UV photodetectors based on ZnO nanofibers. In: *Applied Surface Science*, 2014, 307 pp. 20-3.
29. Zhang, D.H. Adsorption and photodesorption of oxygen on the surface and crystallite interfaces of sputtered ZnO films. In: *Materials Chemistry and Physics*, 1996, 45 (3), pp. 248-52.
30. Xu, K.; Wang, Z.; Wang, F.; Huang, Y.; Wang, F.; Yin, L.; Jiang, C.; He, J. Ultrasensitive Phototransistors Based on Few Layered HfS<sub>2</sub>. In: *Advanced Materials*, 2015, 27 (47), pp. 7881-7.
31. Lupan, O.; Postica, V.; Gröttrup, J.; Mishra, A.K.; De Leeuw, N.H.; Adelung, R. Enhanced UV and ethanol vapour sensing of a single 3-D ZnO tetrapod alloyed with Fe<sub>2</sub>O<sub>3</sub> nanoparticles. In: *Sensors and Actuators B: Chemical*, 2017, 245 pp. 448-61.
32. Peng, S-M.; Su, Y-K.; Ji, L-W.; Wu, C-Z.; Cheng, W-B.; Chao, W-C. ZnO Nanobridge Array UV Photodetectors. In: *The Journal of Physical Chemistry C*, 2010, 114 (7), pp. 3204-8.
33. Debnath, R.; Xie, T.; Wen, B.; Li, W.; Ha, J.; Sullivan, N.F.; Nguyen, N.V.; Motayed, A. A solution-processed high-efficiency p-NiO/n-ZnO heterojunction photodetector. In: *RSC Advances*, 2015, 5 (19), pp. 14646-52.
34. Zhou, X.; Gan, L.; Tian, W.; Zhang, Q.; Jin, S.; Li, H.; Bando, Y.; Golberg, D.; Zhai, T. Ultrathin SnSe<sub>2</sub> Flakes Grown by Chemical Vapor Deposition for High Performance Photodetectors. In: *Advanced Materials*, 2015, 27 (48), pp. 8035-41.
35. Sysoev, V.V.; Schneider, T.; Goschnick, J.; Kiselev, I.; Habicht, W.; Hahn, H.; Strelcov, E.; Kolmakov, A. Percolating SnO<sub>2</sub> nanowire network as a stable gas sensor: Direct comparison of long-term performance versus SnO<sub>2</sub> nanoparticle films. In: *Sensors and Actuators B: Chemical*, 2009, 139 (2), pp. 699-703.
36. Lin, D.; Wu, H.; Zhang, R.; Pan, W. Enhanced Photocatalysis of Electrospun Ag-ZnO Heterostructured Nanofibers. In: *Chemistry of Materials*, 2009, 21 (15), pp. 3479-84.
37. Ren, C.; Yang, B.; Wu, M.; Xu, J.; Fu, Z.; Lv, Y.; Guo, T.; Zhao, Y.; Zhu, C. Synthesis of Ag/ZnO nanorods array with enhanced photocatalytic performance. In: *Journal of Hazardous Materials*, 2010, 182 (1), pp. 123-9.
38. Jin, Y.; Wang, J.; Sun, B.; Blakesley, J.C.; Greenham, N.C. Solution-Processed Ultraviolet Photodetectors Based on Colloidal ZnO Nanoparticles. In: *Nano Letters*, 2008, 8 (6), pp. 1649-53.
39. Michaelson, H.B. The work function of the elements and its periodicity. In: *Journal of Applied Physics*, 1977, 48 (11), pp. 4729-33.